

Journal Pre-proofs

Research paper

An acylhydrazone coumarin as chemosensor for the detection of Ni²⁺ with excellent sensitivity and low LOD: synthesis, DFT calculations and application in real water and living cells

Wen Lu, Jichao Chen, Jiuzhou Shi, Zhong Li, Li Xu, Weina Jiang, Shilong Yang, Buhong Gao

PII: S0020-1693(20)31344-X
DOI: <https://doi.org/10.1016/j.ica.2020.120144>
Reference: ICA 120144

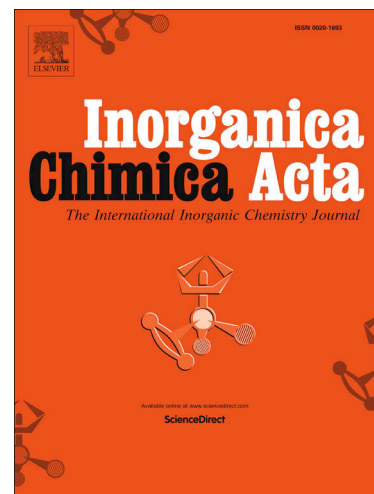
To appear in: *Inorganica Chimica Acta*

Received Date: 17 September 2020
Revised Date: 30 October 2020
Accepted Date: 17 November 2020

Please cite this article as: W. Lu, J. Chen, J. Shi, Z. Li, L. Xu, W. Jiang, S. Yang, B. Gao, An acylhydrazone coumarin as chemosensor for the detection of Ni²⁺ with excellent sensitivity and low LOD: synthesis, DFT calculations and application in real water and living cells, *Inorganica Chimica Acta* (2020), doi: <https://doi.org/10.1016/j.ica.2020.120144>

This is a PDF file of an article that has undergone enhancements after acceptance, such as the addition of a cover page and metadata, and formatting for readability, but it is not yet the definitive version of record. This version will undergo additional copyediting, typesetting and review before it is published in its final form, but we are providing this version to give early visibility of the article. Please note that, during the production process, errors may be discovered which could affect the content, and all legal disclaimers that apply to the journal pertain.

© 2020 Elsevier B.V. All rights reserved.



An acylhydrazone coumarin as chemosensor for the detection of Ni²⁺ with excellent sensitivity and low LOD: synthesis, DFT calculations and application in real water and living cells

Wen Lu,^{a,*,†} Jichao Chen,^{a,†} Jiuzhou Shi,^a Zhong Li,^b Li Xu,^{a,*} Weina Jiang,^a Shilong Yang,^c
Buhong Gao^c

^a College of Science, Nanjing Forestry University, Nanjing 210037, China

^b National Engineering Research Center of Biomaterials, Nanjing Forestry University, Nanjing 210037, China.

^c Advanced Analysis and Testing Center, Nanjing Forestry University, Nanjing 210037, China

[†] These authors contributed equally.

Abstract: A novel acylhydrazone coumarin fluorescent chemosensor **C⁴** for detection of Ni²⁺ was designed and synthesized. The experimental results revealed a low detection limit of 2.1×10^{-11} M with high selectivity and excellent sensitivity towards Ni²⁺. **C⁴** showed a good linear relationship with the concentration of Ni²⁺ from 1.3×10^{-6} to 1.6 μ M. Moreover, a stable complex was formed between **C⁴** and with Ni²⁺ and the binding ratio was proved to be 2: 1 by Job's plot and mass spectrum. The sensing ability of **C⁴** towards Ni²⁺ was attributed to parity-forbidden transition according to fluorescence titrations and DFT calculations. The detection of Ni²⁺ in water samples illustrated **C⁴** could be successfully applied for the detection of Ni²⁺ in real environmental samples. What's more, the fluorescence microscopy images of Hela cells demonstrated the high potential of the novel biosensor for the investigation of biological processes involving Ni²⁺, as well.

Keywords: Coumarin-based chemosensor, Ni²⁺, Low LOD, DFT, Bioimaging

1. Introduction

Nickel is a malleable and ferromagnetic metallic element that can be highly polished. Due to the resistance to corrosion, nickel is widely used in the manufacture of stainless steel and corrosion resistant alloys, as well as for other applications, such as nickel plating, coinage, petroleum, textile, printing, mold and medical treatments [1]. The increased demand for this heavy metal has promoted the extraction of nickel from ores. However, the processes involve in the extraction and utilization are not in accordance with the requirements of environmental protection. As a result, all types of environmental pollution (i.e, air, water, and soil pollution) are already noticed and associated with quantities of nickel above the tolerated limit, which have a negative impact on the human, plants, and animal life [2-3]. Water and soil pollution by nickel harms the ecosystem by reducing, for instance, the crop yield and aquatic products [4-5]. Nickel compounds from the atmosphere can enter the body directly by the respiratory tract, and this excessive intake will generate toxic effects [6-7], such as skin allergy, pulmonary fibrosis, cardiovascular system toxicity, and carcinogenicity (particularly, in nose and kidney) [8-9]. Due to such toxic effects of nickel, the environmental protection agency (EPA) has stipulated that children should not drink water and other beverages containing a concentration of nickel ions higher than 0.04 mg/L [10].

Compared with the traditional analytical methods: Spectrophotometric Method [11-13], Colorimetric Detection [14-15], Flow injection Spectrophotometry [16], Electrochemical Probe [17], Atomic Absorption Spectrometry [18], Reversed-phase High Performance Liquid

Chromatography [19], the fluorescent chemosensors-based methods have attracted particular attention due to its simple operation and convenience alongside with high sensitivity and selectivity [20-28]. A great many efforts have been paid for designing and synthesizing sensors with high selectivity, sensitivity, low detection limit and instantaneous response [29-31]. Many fluorescent sensors for highly sensitive sensing Ni^{2+} have been widely reported with enhancement of fluorescence [32-35]. Besides, a pyrazolopyrimidine-derived fluorescent chemosensor with high sensitivity and selectivity towards Ni^{2+} has been developed based on intramolecular charge transfer (ICT) which revealed fluorescence quenching [36]. Moreover, acridine derived-fluorescent sensor was used to construct a novel chemosensor for Ni^{2+} detection at low concentrations [37]. As we know, the concentration of nickel in natural freshwater is about 0.5 $\mu\text{g/L}$ (8.5×10^{-9} M), while the lowest LOD for Ni^{2+} in these reports is 2.16×10^{-8} M [29]. In this work, we further reduce the LOD to 2.1×10^{-11} M, which will broaden the detection range for nickel ion application in environmental protection, biology, and medicine.

Coumarin is a natural product found in black vanilla, wild vanilla, chamomile, and orchid. Coumarin has high fluorescence quantum yield, large Stock's shift, adjustable photophysical and photochemical properties, and good light stability [34]. As a result, coumarin has been developed as a fluorescent chemosensor for the detection of various ions and molecules [38-47].

We synthesized a coumarin acylhydrazone-based fluorescent chemosensor, **C⁴** ((E)-N¹-(2-chloro-6-hydroxybenzylidene)-7-(diethylamino)-2-oxo-2H-chromene-3-carbohydrazide), to detect Ni^{2+} . The photo-physical properties of **C⁴** chemosensor for Ni^{2+} were studied in details by fluorescence spectroscopy, absorption spectroscopy, and confocal fluorescence imaging. The high sensitivity of this new sensor was proved by the low detection limit of 2.1×10^{-11} M. In addition, it proved to be highly selective for Ni^{2+} based on the experiments performed in the presence of other di- and trivalent cations.

2. Experimental

2.1. Characterization

UV-vis and fluorescent spectra were recorded on a LAMBDA950 spectrometer (Perkin Elmer Precisely) and a LS 55 Fluorescence Spectrometer (Perkin Elmer), respectively, using a 1-cm square quartz cell. The excitation wavelength of 426 nm (excitation/emission slit widths = 12 nm / 2.5 nm) was used for all measurements. ^1H and ^{13}C NMR spectra were recorded on a Bruker AVANCE III HD spectrometer operating at 600 MHz. Mass spectrometry was recorded on the LTQ-Orbitrap (Thermo Fisher Scientific). The live-cell imaging of HeLa cells was performed on a Zeiss LSM710 Airyscan confocal laser scanning microscope.

2.2. Synthesis of **C⁴**

Compound **2** (0.55 g, 2 mmol) and 2-chloro-6-hydroxybenzaldehyde (0.33 g, 2 mmol) were dissolved in 20 mL anhydrous ethanol and refluxed for 6 h. After cooling to room temperature, the yellow solid formed was washed with ethanol to obtain **C⁴** (0.7954 g, 96%). ^1H NMR (600 MHz, $\text{DMSO-}d_6$) δ (ppm) : 12.60 (s, 1H, NH), 12.07 (s, 1H, Ar-OH), 9.11 (s, 1H, CH=N), 8.74 (s, 1H, C=CH), 7.73 (d, 1H, Ar-H, $J=8.4$ Hz), 7.32 (t, 1H, Ar-H, $J=7.8$ Hz), 7.04 (d, 1H, Ar-H, $J=7.8$ Hz), 6.94 (d, 1H, Ar-H, $J=8.4$ Hz), 6.85 (d, 1H, Ar-H, $J=9.0$ Hz), 6.68 (s, 1H, Ar-H), 3.53~3.32 (m, 4H, CH_2), 1.16 (t, 6H, CH_3 , $J=7.2$ Hz). ^{13}C NMR (150 MHz, $\text{DMF-}d_7$) δ (ppm): 161.70, 160.49,

159.90, 158.38, 153.76, 149.30, 147.34, 134.30, 132.38, 120.66, 116.58, 116.02, 110.87, 108.64, 108.58, 96.47, 45.04, 12.31. ESI-MS m/z : 436.1034 [C^4+Na]⁺.

2.3. Preparation of stock solution of C^4 and metal ions

All reagents used in this work were purchased from professional commercial suppliers and were used directly without further purification. The solutions of metal ions were prepared from salts of $AlCl_3 \cdot 6H_2O$, $Ca(CH_3COO)_2 \cdot H_2O$, $Cd(CH_3COO)_2 \cdot 2H_2O$, $CoCl_2 \cdot 6H_2O$, $Cr(CH_3COO)_3$, $CuCl_2 \cdot 2H_2O$, $FeCl_2 \cdot 4H_2O$, $FeCl_3 \cdot 6H_2O$, CH_3COOK , $Mg(CH_3COO)_2 \cdot 4H_2O$, $Mn(CH_3COO)_2 \cdot 4H_2O$, $Ni(CH_3COO)_2 \cdot 4H_2O$, $Pb(CH_3COO)_2 \cdot 3H_2O$ and $Zn(CH_3COO)_2 \cdot 2H_2O$ in deionized water with a concentration of 10^{-3} M. The solution of C^4 chemosensor (1.0 mM) was dissolved in different solvents (THF, DMF and DMSO). For the fluorescence spectra measurements, a concentration of 1.0 μM C^4 (THF: PBS=99:1, v/v) was used while UV-vis spectra measurements were performed with a C^4 solution with a concentration of 10.0 μM (THF: PBS=99:1, v/v).

2.4. Limit of detection (LOD)

The limit of detection (LOD) and binding stoichiometry were evaluated based on fluorescence titrations. A plot of the measured fluorescence intensity at the emission band 462.5 nm versus concentration of Ni^{2+} was constructed to evaluate the limit of detection based on the equation $LOD = 3\sigma/k$, where σ is the standard deviation of the emission of a blank solution and k is the slope of the calibration curve. Each measurement was performed three times [48-49].

2.5. Computational methodology

Density functional theory (DFT), model B3LYP [50-51], has been used to optimize the geometric structures of C^4 molecule and C^4 -Ni (II) complex in the lowest singlet spin state S_0 . The geometries for the first excited singlet states S_1 of C^4 were optimized with TD-PBE0 method to obtain their fluorescence emission energies and spectra. To analyze the nature of fluorescence emission, natural transition orbital (NTO) method was applied based on the TDDFT calculations [52]. In all calculations, the solvation effect was evaluated based on the SMD solvation model [53], the energies were computed with the 6-31G* basis set for C, H, N, and O atoms and the SDD effective core potential for Ni atom. All calculations were performed with Gaussian 09 program.

2.6. Detection of Ni^{2+} in water samples

Water samples used in this work were ultrapure water and tap water from the Nanjing Forestry University. Different concentrations of Ni^{2+} (0.1, 0.2 0.3 μM in ultrapure water and 0.2, 0.4, 0.6 μM in tap water) and C^4 chemosensor (1 μM) were used for the measurements (pH=6.8-7.4). The fluorescence intensity at 462.5 nm was then measured, and each sample was tested three times.

2.7. Cell cytotoxicity study

The survival rate and toxicity of HeLa for C^4 was measured by MTT. Logarithmically grown HeLa cells (90% DMEM, 10% FBS, 5% Penicillin-Streptomycin Solution) were inoculated into 96-well plates at 10000 per well and incubated in incubator (37°C, 5% CO_2) for 24 h. After then, the medium was removed and washed with PBS for three times. 100 μL of C^4 (The termination concentration was 0.01-100 μM) was added, culturing the cell at 37°C, 5% CO_2 for another 24 h.

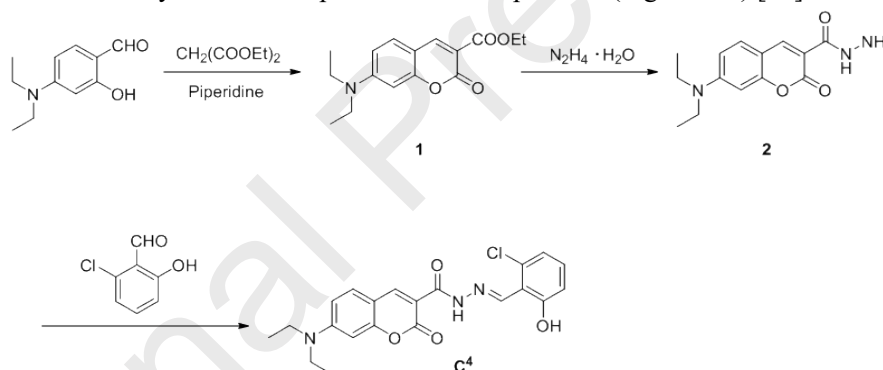
Similarly, the medium was removed, washed with PBS for three times, and 100 μL of MTT (1mg/mL) was added to culture for 12 h. Removing the supernatant, adding 150 μL of DMSO to each hole, and testing the absorbance at 590 nm with Filter Max F5 (MD, American). Repeat the experiment ten times and take the average.

2.8. Cell imaging study

Hela cells were used for cell imaging. The medium contained 10% FBS and 5% penicillin-streptomycin mixed solution. The samples were incubated at 37 $^{\circ}\text{C}$ in 5% CO_2 . Hela cells were inoculated in 6 well plates with coverslip and 1.5×10^4 cells per well. After 24 h, the medium was removed and the cells washed three times with PBS (pH = 7.2). Then, the C^4 ligand (1×10^{-5} M) was added to the cells followed by incubation for 1 h. At the end of the process, the medium was removed and the cells washed three times with PBS. Finally, 5×10^{-5} M Ni^{2+} solution was added and co-incubated for 1 h. The cover glass was washed three times with PBS and double steamed water. The fluorescence of cells was observed by confocal laser scanning fluorescence microscopy.

3. Results and discussion

The C^4 ligand was synthesized by a condensation reaction between a coumarin-based molecule (compound **1**) and 2-chloro-6-hydroxybenzaldehyde, as described in Scheme 1. The method of the reference was used to synthesize compound **1** and compound **2** (Fig. S1-S7) [43].



Scheme 1. The reaction involved in the synthesis of C^4 .

3.1. Sensing properties of C^4 chemosensor for Ni^{2+}

First, the role played by solvent on the spectral properties of C^4 was evaluated. According to the solubility of C^4 , DMF, DMSO and THF were chosen for these tests. Hence, different solvents (THF, DMF, and DMSO) were selected to prepare C^4 solution of 10 μM and 1 μM , and then the UV-vis absorbance and fluorescence emission spectra were recorded respectively (Fig. S8). It can be seen there is no obvious difference between the absorbance intensity for the molecule dissolved in DMF, DMSO and THF. For the fluorescence properties, the effect of the solvent is more obvious. The fluorescence emitted by C^4 dissolved in THF was much stronger in comparison with those emitted in DMF and DMSO. As the proportion of water in the solution increased, both absorption and fluorescence intensity decreased. This may be caused by the decrease in solubility of C^4 with the addition of water, which favored the molecular aggregation. On the basis of UV-vis absorption and fluorescence emission spectra, the best solvent was THF and it was used for further investigations.

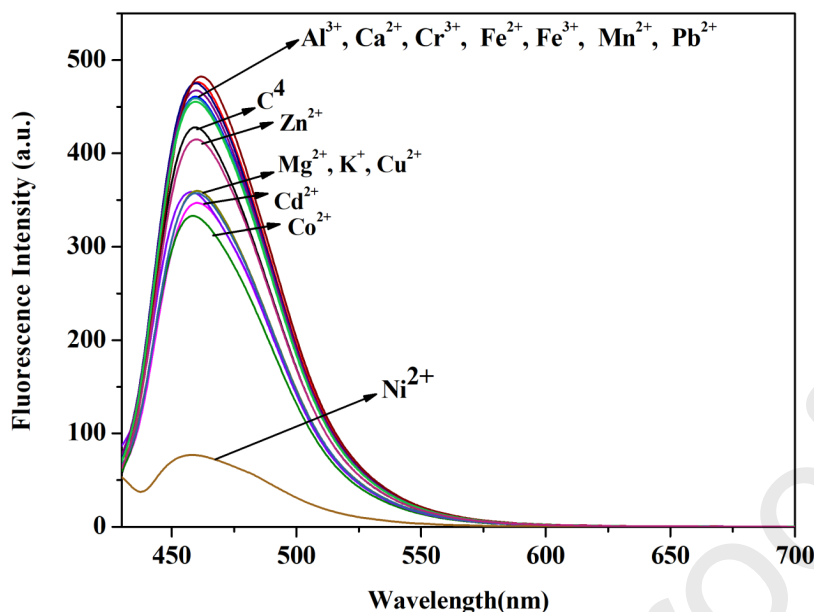


Fig. 1. Fluorescence spectra of C^4 in the presence of different metal ions (THF: PBS=99:1, v/v, $\lambda_{ex} = 426$ nm, slit width = 12, 2.5 nm).

To evaluate the selectivity of C^4 towards Ni^{2+} , several metal ions (Al^{3+} , Ca^{2+} , Cd^{2+} , Co^{2+} , Cr^{3+} , Cu^{2+} , Fe^{2+} , Fe^{3+} , K^+ , Mg^{2+} , Mn^{2+} , Na^+ , Ni^{2+} , Pb^{2+} and Zn^{2+}) were added to the C^4 solution and then the fluorescence was recorded. For this test, 1 equiv. metal ions was used. As the experimental results displayed in Fig. 1 show, only Ni^{2+} has an obvious fluorescence response. The color of solution turned dark yellow from bright yellow with addition of Ni^{2+} (Color change induced by the addition of Ni^{2+} was seen in Fig. 2). The fluorescence intensity of the C^4 solution with addition of Ni^{2+} quenched.

To evaluate the binding ability of C^4 to Ni^{2+} , fluorescence titration profiles of C^4 were carried out by increasing the amounts of Ni^{2+} in the solution, as shown in Fig. 2. With increasing the concentration of Ni^{2+} , the intensity of the emitted fluorescence of C^4 at 462.5 nm gradually decreased. The lowest and stable fluorescence signal was obtained and a good linearity was obtained in the range in the fluorescence intensity in the concentration range of $1.3 \times 10^{-6} - 1.6 \mu M Ni^{2+}$ ($R^2 = 0.99238$) according to $LOD = 3\sigma/k$ (σ was shown in Table S1). To note, the limit of detection was of 2.1×10^{-11} M, which is lower than that reported for other chemosensors. For example, in Ghazali's article, the LOD was 2.16×10^{-8} M [29] and 8.3×10^{-8} M [30] in Velmurugan's article. Many reported chemosensors's LOD was higher than LOD in this paper (Table 1).

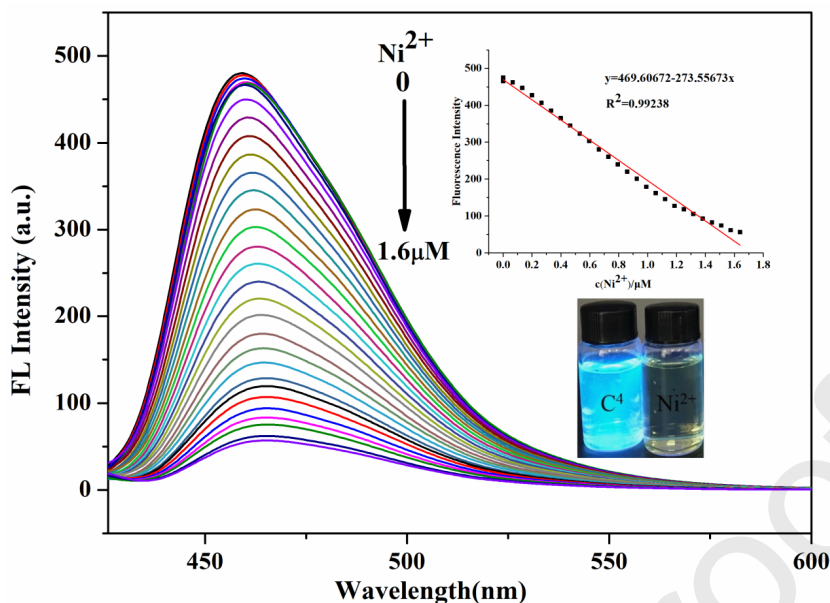


Fig. 2. Standard curve for fluorescence emission intensity vs Ni^{2+} concentration ($\lambda_{\text{exc}} = 426$ nm, slit width = 12, 2.5 nm). Inset: Color change induced by the addition of Ni^{2+} (1 equiv.) to the solution of C^4 ($\text{C}^4 = 1 \times 10^{-6}$ mol/L, THF: PBS=99:1, v/v).

3.2. Metal ion selectivity study

To investigate the practical utility of the synthesized C^4 chemosensor, competitive titration was performed in the presence of various metal ions, i.e., Al^{3+} , Ca^{2+} , Cd^{2+} , Co^{2+} , Cr^{3+} , Cu^{2+} , Fe^{2+} , Fe^{3+} , K^+ , Mg^{2+} , Mn^{2+} , Pb^{2+} and Zn^{2+} . For these experiments, the concentration of interfering ions was four times higher than that of C^4 . The results, expressed as fluorescence intensity versus the composition of the sensing solution, are displayed in Fig. 3. It is obvious that irrespective of the initial fluorescence intensity, it is quenched when Ni^{2+} is added to the “ C^4 + interfering ion” solution. Interestingly, the level of quenching is similar in all cases, which indicates the high affinity of the sensor for Ni^{2+} . These results clearly show that the developed chemosensor is highly selective for the detection of Ni^{2+} .

Furthermore, to examine the stability of the C^4 chemosensor, the solution of C^4 and C^4 -Ni (II) was kept for a period of 48 hours and the fluorescence was measured at different intervals of time. As shown in Fig. 4, the intensity of fluorescence keeps constant over the entire period which means that the chemosensor was stable.

Table 1. Comparison of the reported sensors for Ni^{2+} .

Target	LOD (M)	Ref.
Ni^{2+}	2.16×10^{-8}	29
	3.80×10^{-8}	36
	8.30×10^{-8}	54
	3.61×10^{-7}	31
	1.52×10^{-6}	37
	1.91×10^{-6}	55
	4.91×10^{-6}	30
	1.00×10^{-5}	56
	9.30×10^{-4}	57

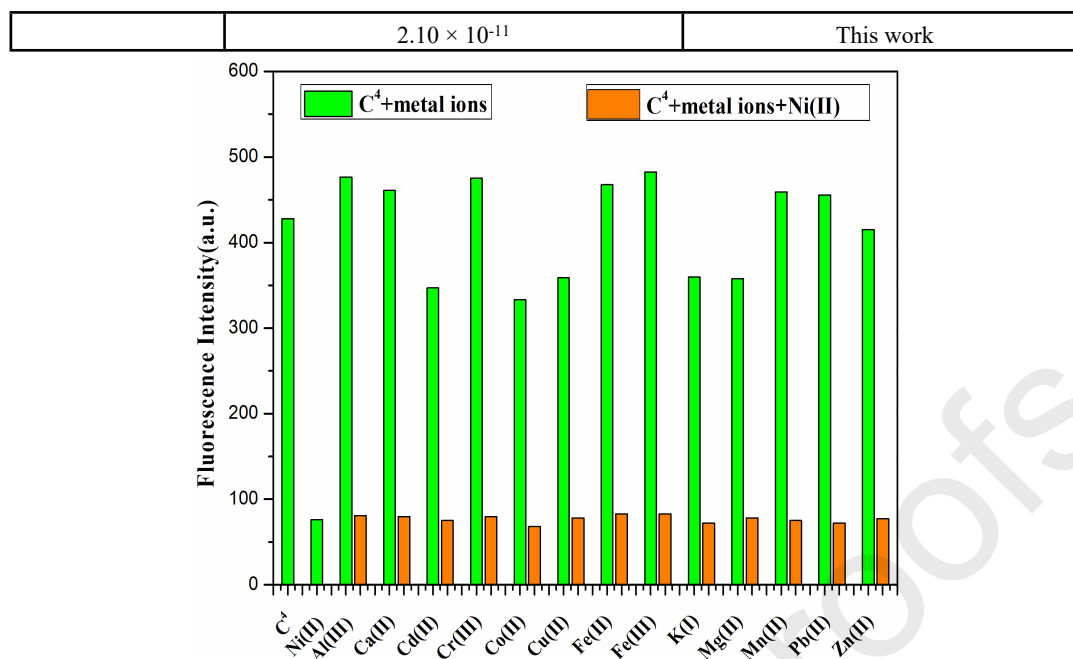


Fig. 3. Fluorescence spectra of C^4 in the presence of interfering metal ions (C^4 =metal ions= 1×10^{-6} mol/L, THF: PBS=99:1, v/v.).

3.3. Binding stoichiometry

To assess the binding stoichiometry between the prepared C^4 sensor and Ni^{2+} , Job's plot of fluorescence emission was recorded at different ratio of C^4 and Ni^{2+} . As shown in Fig. 5, the result demonstrated a ratio of 2:1 between C^4 and Ni^{2+} ion.

The binding ability between C^4 and Ni^{2+} ion was measured by Stern-Volmer equation [58] which is often used in quenched chemosensor.

$$F_0/F = 1 + K_{sv}\tau_0[Q] = 1 + K_{sv}[Q]$$

Here, F_0 is the fluorescence intensity of chemosensor in the absence of quenching agent, F is the fluorescence intensity recorded in the presence of quenching agent, K_{sv} is constant of Stern-Volmer, $[Q]$ is the concentration of quenching agent which is $[Ni^{2+}]$. The constant K_{sv} could be determined from the slop of the straight line of the plot of F_0/F against $[Q]$. The K_{sv} was calculated to be $2 \times 10^6 M^{-1}$. And the result confirmed the chemosensor had an excellent binding ability between C^4 and Ni^{2+} ion.

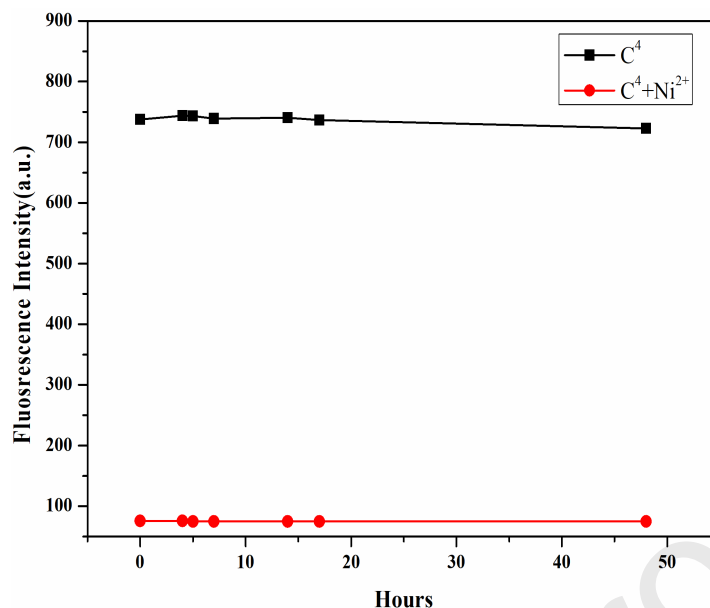


Fig. 4. Fluorescence spectra of C⁴-Ni (II) complex at different intervals of time.

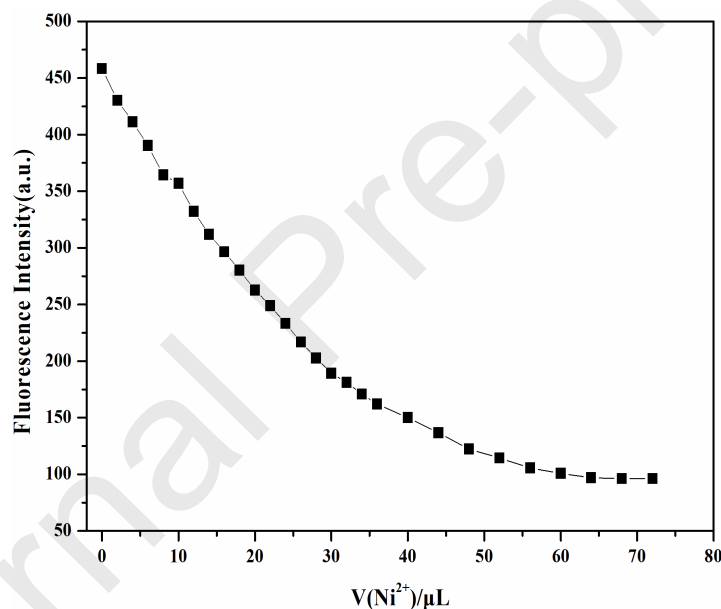


Fig. 5 Job's plot of C⁴-Ni²⁺ complex in THF: PBS=99:1, v/v.

3.4. Mass spectrometry studies

The binding mode of C⁴ with Ni²⁺ was analyzed by mass spectrometry, as well (Fig. 6a). The mass fraction at $m/z = 413.1142$ belongs to free C⁴ ligand, whereas the mass fraction at $m/z = 883.1544$ is associated with the complex formed between ligand and metal ion, $[\text{Ni}(\text{C}^4)_2+\text{H}]^+$, in the stoichiometric ratio of 2 : 1 $m/z=436.1027$ was the ion peak of $[\text{C}^4+\text{Na}]^+$. The chemical formula of the complex is $\text{C}_{42}\text{H}_{39}\text{O}_8\text{N}_6\text{Cl}_2\text{Ni}$. In addition, the experimental spectrum is in line with the simulated one, as shown in Fig. 6b.

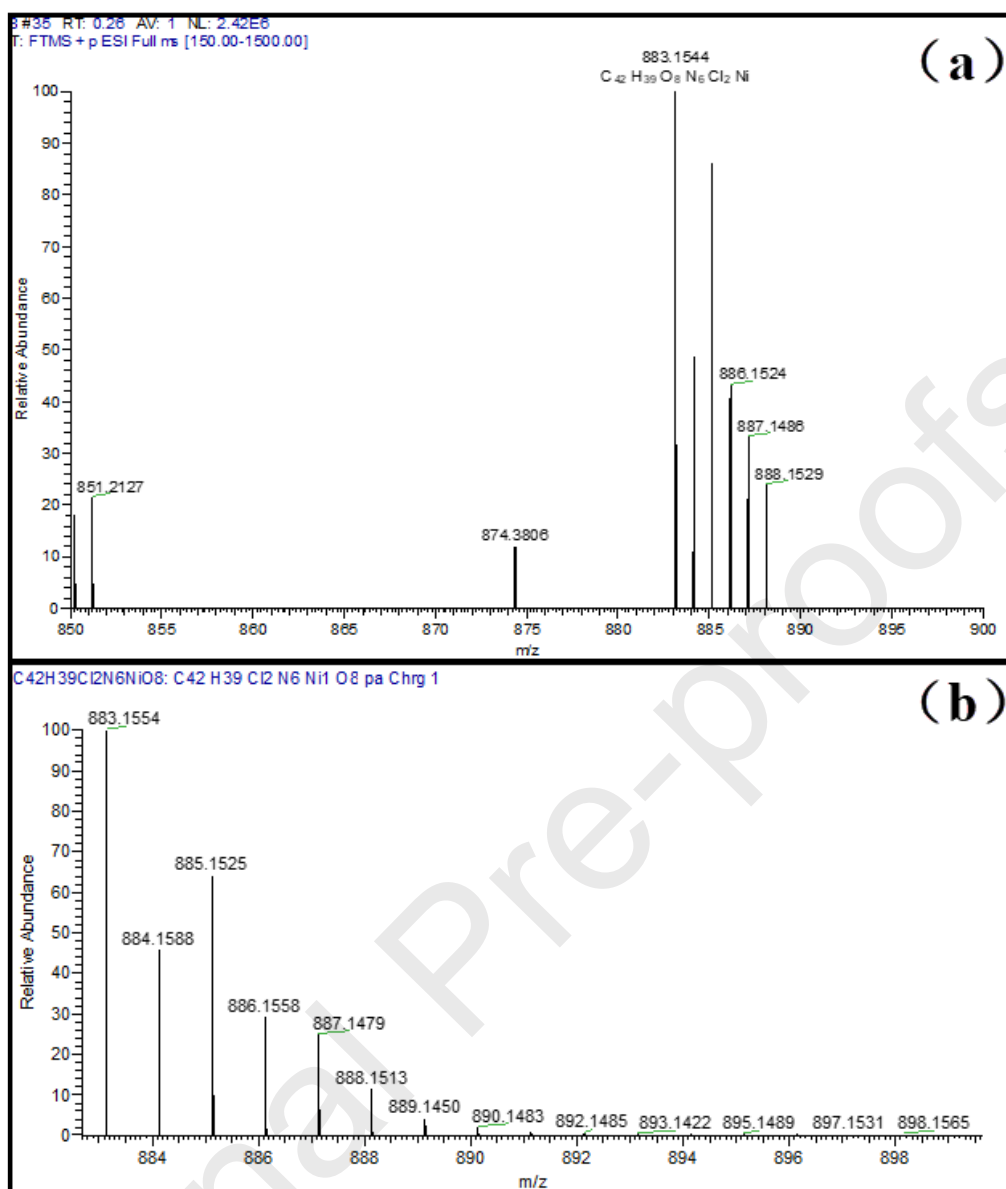


Fig. 6. Experimental (a) and simulated mass spectrum (b) of $C^4-Ni(II)$.

3.5. Theoretical calculation studies

According to the Job plot, fluorescence titration, and ESI-mass analysis, we proposed the possible structure of 2: 1 $C^4-Ni(II)$ complex. The computational study was performed by using the density functional theory (DFT) and time dependent density functional theory (TDDFT) methods in parallel with the natural transition orbital (NTO) method to gain further insight into the 'turn off' mechanism of C^4 sensor.

The theoretical results confirmed the energy and the charge transfer model proposed to explain the mechanism of the fluorescence quenching. According to Kasha's rule, the fluorescence is generated when the electrons are transferred from S_1 to S_0 . We calculated the vertical electronic S_1 to S_0 transitions of C^4 and $C^4-Ni(II)$ by TDDFT method. Table S2 display the orbital pairs involved in the electronic transition and accountable for the intense fluorescence emission of C^4 and $C^4-Ni(II)$ complex. Clearly, the electronic transition of C^4 molecule is a Local Excitation (LE), C^4 having a $S_0 \rightarrow S_1$ excitation energy of 2.7624 eV (448.83 nm) and an oscillator strength of

1.7219, which could be attributed to the intense absorption. In addition, the theoretical absorption at 448.8 nm ($S_0 \rightarrow S_1$ excitation) of C^4 is in well agreement with the experimental absorption of 462.5 nm while the dominant MO transition is MO108 \rightarrow MO109. C^4 -Ni(II) has a $S_0 \rightarrow S_1$ excitation energy of 0.8253 eV and an oscillator strength of 0.0001 which inferred to parity-forbidden. Yet, no dominant MO transition was observed for C^4 -Ni(II), the largest contribution of a single MO pair is only of 26.71%, which makes it impossible to identify the nature of this excitation based on MO pair only. Therefore, the natural transition orbital (NTO) distribution of the complex C^4 -Ni(II) was calculated. As shown in Fig. 7, the optical emissions are mainly attributed to the d-d orbital transitions in Ni atom from NTO224 to NTO225.

To summarize, the computational results along with the experimental data were demonstrated the complex formation between C^4 and Ni^{2+} . In addition, it is confirmed that the fluorescence quenching in the presence of Ni^{2+} may due to the parity-forbidden transition according to the Laporte selection rule.

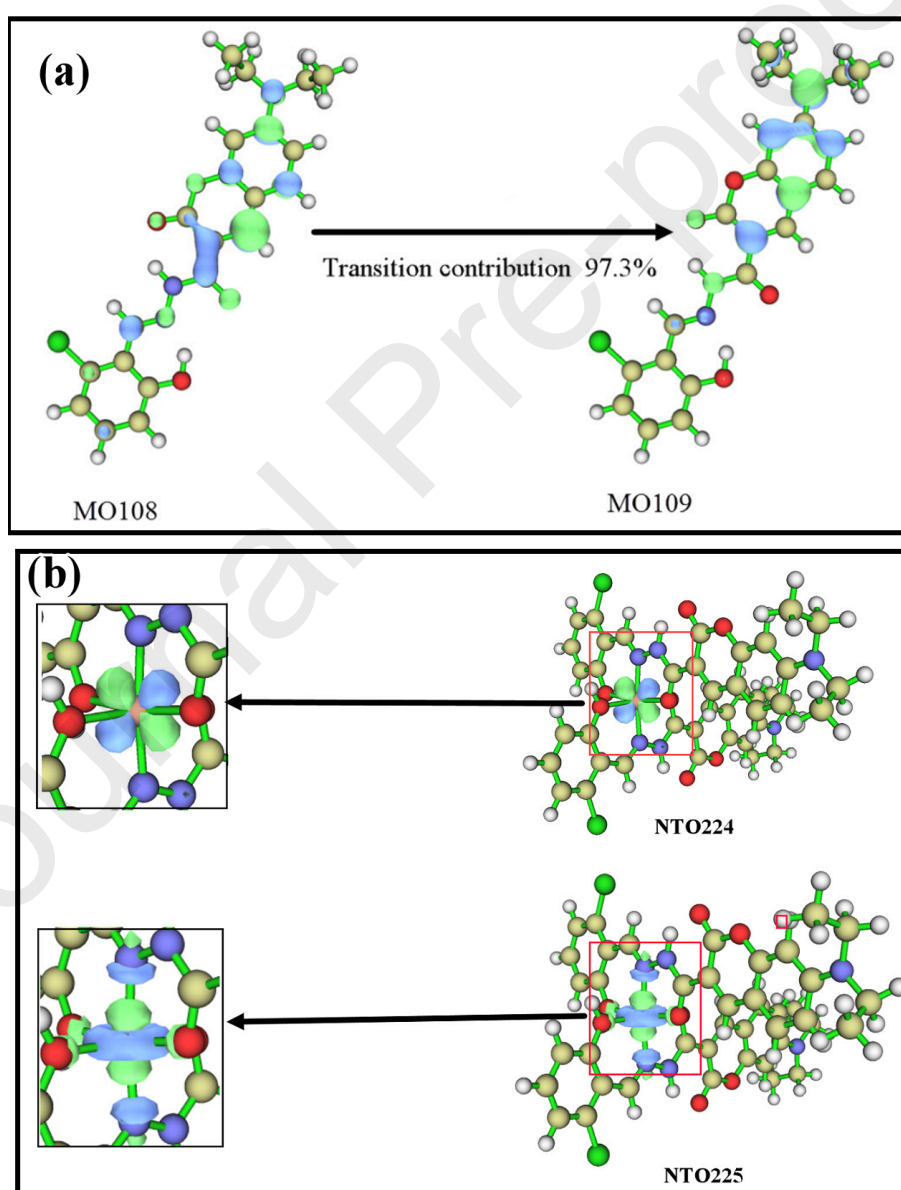


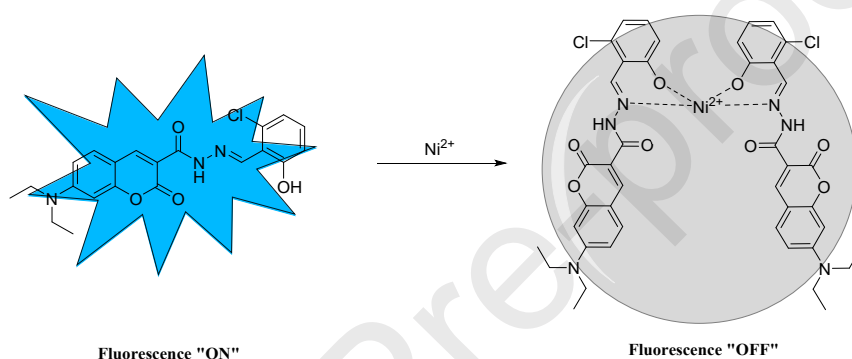
Fig. 7 (a) The orbitals involved in the principal electronic transition $S_0 \rightarrow S_1$ of C^4 ; (b) Dominant natural transition orbital (NTO) pairs of the principal electronic transition $S_0 \rightarrow S_1$ in C^4 -Ni(II).

3.6. The proposed binding mechanism

Based on the results of mass spectrometry, and DFT studies, the possible binding mechanism in C^4 -Ni (II) complex is shown in Scheme 2. Ni^{2+} coordinated to the phenolic hydroxyl of salicylaldehyde and N atom in C=N Schiff base. N atom in C=N is a perfect coordination atom and often be used to coordinate with metal ions [69-63]. As a result, the fluorescence is quenched [64-65] and the coordination mode is similar to reported work [60].

3.7. Application of C^4 for detection of Ni^{2+} in water samples

To prove the practical application of C^4 for Ni^{2+} detection, experiments were carried out with ultrapure and real water samples. In the linear range of Ni^{2+} concentration, water sample was spiked with standard Ni^{2+} solution at different concentrations. The results showed good values for the recovery and relative standard deviation (R.S.D.), which proved the ability of the chemosensor to successfully detect Ni^{2+} in environmental samples (Table 2).



Scheme 2. Proposed mechanism for detection of Ni^{2+} by C^4 .

Table 2. Determination of Ni^{2+} in water samples from different sources.

Sample	Added (μM)	Found (μM)	Recovery (%)	RSD (%)
Ultrapure water	0.10	0.10	101.11 \pm 0.29	2.91
	0.20	0.19	98.10 \pm 0.34	1.75
	0.30	0.31	100.74 \pm 0.27	0.91
Tap water	0.20	0.21	104.34 \pm 0.61	2.95
	0.40	0.44	109.68 \pm 0.56	1.28
	0.60	0.62	103.14 \pm 0.90	1.46

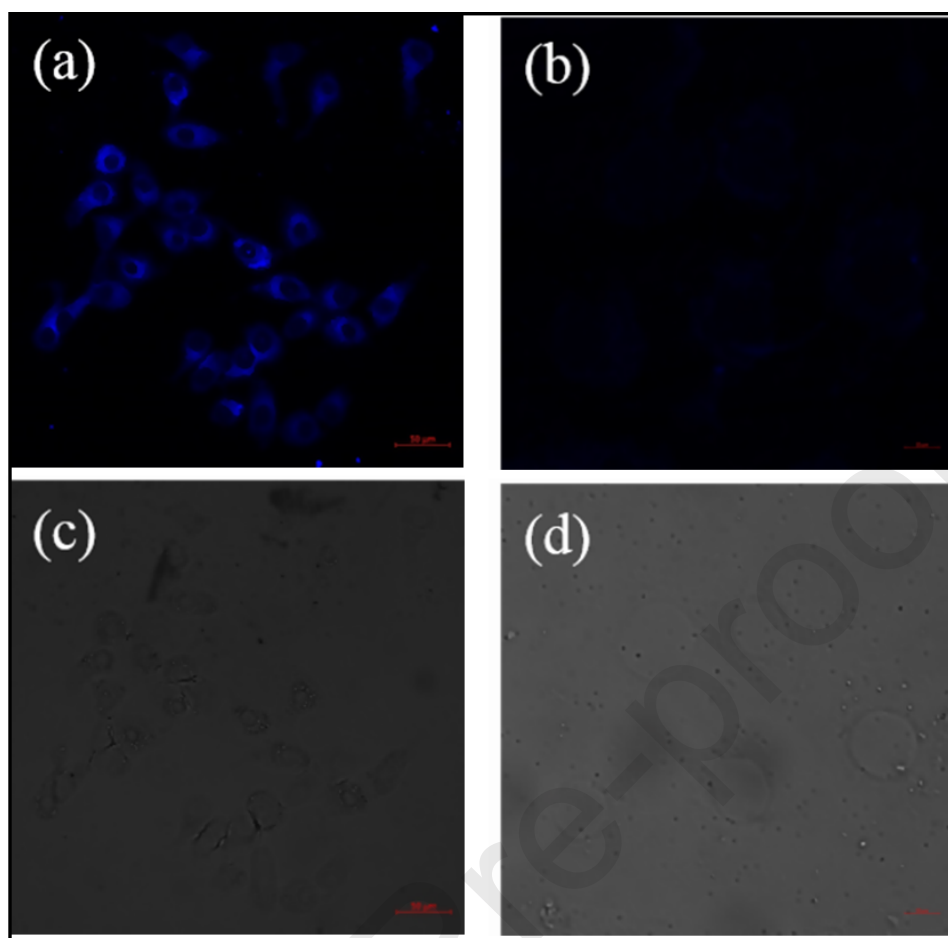


Fig. 8. Fluorescence images of HeLa cells incubated with C^4 (10 μ M) (a), further incubated with Ni^{2+} (50 μ M) (c), and their corresponding bright field images (b, d).

3.8. Cell cytotoxicity study and cell image experiment

We further investigated the fluorescence imaging in HeLa cells treated with C^4 (10 μ M) for 12 h. Before carrying out the cell image experiment, the cell cytotoxicity of C^4 was performed by MTT. The IC_{50} of C^4 with HeLa cells is 21.83 after incubating for 12 hours, meaning C^4 is low toxicity to HeLa cells and could be used for bioimaging. As shown in Fig. 8, a strong blue fluorescence was observed with addition of C^4 into HeLa cells (Fig. 8a). Then, Ni^{2+} (50 μ M) was added and incubated for 1 h, and a fluorescence emission can be observed, but of much lower intensity in comparison with the sample without Ni^{2+} (Fig. 8c). This indicates that the cell membrane excellent permeability for C^4 , which once internalized in the cell can detect exogenous Ni^{2+} .

4. Conclusion

In summary, a new coumarin-based selective and sensitive chemosensor for Ni^{2+} ion detection was developed and characterized by NMR, and ESI-MS techniques. This chemosensor exhibited a turn-off fluorescence response towards Ni^{2+} , whose intensity was quenched in the presence of this ion. The detection limit was as low as 2.1×10^{-11} M. The sensor also selectively recognized Ni^{2+} in the presence of various competing ions. According to fluorescence titrations, and DFT calculations, the sensing ability of C^4

towards Ni²⁺ was attributed to parity-forbidden transition. The binding stoichiometry between C⁴ and Ni²⁺ was of 2: 1. The new developed ligand proved to be a good chemosensor for detection of Ni²⁺ in real water samples. In addition, the bio-imaging of Hela cells demonstrated the permeability of the cell membrane for C⁴ followed by the detection of Ni²⁺, demonstrating the possible utility in sensing of Ni²⁺ in living cells.

Acknowledgements

This work was supported by the National Key Research and Development Program of China (2017YFD060070602), Innovation Fund for Young Scholars of Nanjing Forestry University (CX2017017, CX2017004), and the priority academic program development of Jiangsu higher education institutions.

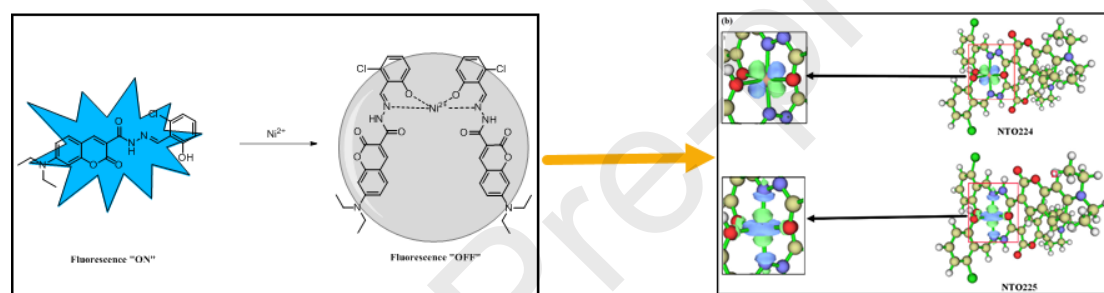
References

- [1] D.J. Xing, W. Liu, S.H. Guo, X.F. Kang, S.J. Li, Z.J. Qiu, X.Z. Yu, *Maternal and Child Health Care of China* 31 (2016) 929-931.
- [2] S.C. Dodani, Q. He, C.J. Chang, *J. Am. Chem. Soc.* 131 (2009) 18020-18021.
- [3] Y. Jeong, J. Yoon, *Inorg. Chim. Acta* 381 (2012) 2-14.
- [4] A.Q. Pan, *J. Clin. Med.* 19 (2015) 179-180.
- [5] S.J. Zhang, Hebei Medical University (2016).
- [6] M.J. Wu, *Studies of Trace Elements and Health* 31 (2014) 74-75.
- [7] H. Babich, G. Stotzky, *Adv. Appl. Microbiol.* 29 (1983) 195-265.
- [8] E. Denkhaus, K. Salnikow, *Crit. Rev. Oncol. Hemat.* 42 (2002) 35-56.
- [9] T.P. Coogan, D.M. Latta, E.T. Snow, M. Costa, A. Lawrence, *CRC Critical Reviews in Toxicology* 19 (1989) 341-384.
- [10] US Department of Health and Human Services, *Public Health Service* (1996).
- [11] B.B.A. Francisco, L.F.S. Caldas, D.M. Brum, R.J. Cassella, *J. Hazard. Mater.* 181 (2010) 485-490.
- [12] V.N. Bulut, D. Arslan, D. Ozdes, M. Soylak, M. Tufekci, *J. Hazard. Mater.* 182 (2010) 331-336.
- [13] A. Shahryar, F. Abbas, B.G. Mohammad, N. Ali, A. Freshteh, K. Hossein, *Food Chem.* 116 (2009) 1019-1023.
- [14] Y.L. Hung, T.M. Hsiung, Y.Y. Chen, Y.F. Huang, C.C. Huang, *J. Phys. Chem. C* 114 (2010) 16329-16334.
- [15] S. Tontrong, S. Khonyoung, J. Jakmunee, *Food Chem.* 132 (2012) 624-629.
- [16] J. Herdan, R. Feeney, S.P. Kounaves, A.F. Flannery, C.S. Stormont, G.T.A. Kovacs, R.B. Darling, *Environ. Sci. Technol.* 32 (1998) 131-136.
- [17] H.N. Kim, W.X. Ren, J.S. Kim, J. Yoon, *Chem. Soc. Rev.* 41 (2012) 3210-3244.
- [18] H. Sang, P. Liang, D. Du, *J. Hazard. Mater.* 154 (2008) 1127-1132.
- [19] H.Z. Lian, Y.F. Kang, S.P. Bi, Y. Aekin, D.L. Shao, D.N. Li, Y.J. Chen, L.M. Dai, N. Gan, L. C. Tian, *Talanta* 62 (2004) 43-50.
- [20] J.F. Zhang, Y. Zhou, J. Yoon, S.K. Jong, *Chem. Soc. Rev.* 42 (2011) 3416-3429.
- [21] C.C. Chang, F. Wang, T.W. Wei, X.Q. Chen, *Ind. Eng. Chem. Res.* 56 (2017) 8797-8805.
- [22] S.H. Lee, H.J. Kim, Y.O. Lee, J. Vicens, J.S. Kim, *Tetrahedron Lett.* 47 (2006) 4373-4376.
- [23] G.F. Wu, M.X. Li, J.J. Zhu, K.W.C. Lai, Q. Tong, F. Lu, *RSC Adv.* 6 (2016) 100696-100699.
- [24] S.Y. Qin, B. Chen, J. Huang, Y.F. Han, *New J. Chem.* 42 (2018) 12766-12772.
- [25] B. Qiu, Y. Zeng, R. Hu, L.Y. Chen, J.P. Chen, T.J. Yu, G.Q. Yang, Y. Li, *ACS Omega* 3 (2018) 18153-18159.

- [26] D. Udhayakumari, S. Saravanamoorthy, M. Ashok, S. Velmathi, *Tetrahedron Lett.* 52 (2011) 4631-4635.
- [27] F. Song, C. Yang, H.B. Liu, Z.G. Gao, J. Zhu, X.F. Bao, C. Kan, *Analyst* 144 (2019) 3094-3102.
- [28] F. Song, C. Yang, X.T. Shao, L. Du, J. Zhu, C. Kan, *Dyes Pigments* 165 (2019) 444-450.
- [29] S. Ghazali, J. L. Fan, J. J. Du and X. J. Peng, *Methods* 168 (2019) 24-28.
- [30] K. Velmurugan, J.P. Raman, A.N. Duraipandy, M.S. Kiran, S. Easaramoorthi, L.J. Tang, R. Nandhakumar, *ACS Sustain. Chem. Eng.* 6 (2018) 16532-26543.
- [31] G.V.K. Gajuluva, P.K. Mookkandi, S. Murugesan, S. Kathiresan, R. Jegathalaprathaban, S. Gandhi, *New J. Chem.* 42 (2018) 2865-2873.
- [32] G.X. Yin, J.F. Yao, S. Hong, Y.N. Zhang, Z.H. Xiao, T. Yu, H.T. Li, P. Yin, *Analyst* 144 (2019) 6962-6967.
- [33] M.Q. Liu, Z.P. Yin, Y.X. Tan, J.H. Li, H. Peng, A. Duan, C.H. Luo, *Dyes Pigments* 181 (2020) 108582.
- [34] M. Dhanushkodia, G.G.V. Kumar, B.K. Balachandar, S. Sarveswari, S. Gandhi, J. Rajesh, *Dyes Pigments* 173 (2020) 107879.
- [35] K. Velmurugan, J. Prabhu, A. Raman, N. Duraipandy, M.S. Kiran, S. Easwaramoorthi, L.J. Tang, R. Nandhakumar, *Acs Sustain. Chem. Eng.* 6 (2018) 16532-16543.
- [36] Y.Q. Gu, W.Y. Shen, Y. Zhou, S.F. Chen, Y. Mi, B.F. Long, D.J. Young, F.L. Hu, *Spectrochim. Acta A* 209 (2019) 141-149.
- [37] C.Y. Wang, J.X. Fu, K. Yao, K. Xue, K.X. Xu, X.B. Pang, *Spectrochim. Acta A* 199 (2018) 403-411.
- [38] W.H. Ma, X.J. Peng, Q. Xu, B. Song, *Prog. Chem.* 19 (2007) 1258-1266.
- [39] Z.J. Hu, J.W. Hu, H. Wang, Q. Zhang, M. Zhao, C. Brommesson, Y.P. Tian, H.W. Gao, X.J. Zhang, K. Uvdal, *Anal. Chim. Acta* 933 (2016) 189-195.
- [40] Y.X. Ma, Y. Zhao, L.L. Xia, J.X. Huang, Y.Q. Gu, P. Wang, *Anal. Chim. Acta* 1035 (2018) 161-167.
- [41] S. Biswas, M. Gangopadhyay, S. Barman, J. Sarkar, N.D.P. Singh, *Actuat. B-Chem.* 222 (2016) 823-828.
- [42] K. Wang, L. Ma, G. Liu, D. Cao, Z. Liu, *Dyes and Pigments* 26 (2016) 104-109.
- [43] G.J. He, J. Li, Z.Q. Wang, C.X. Liu, X.L. Liu, L.G. Ji, C.Y. Xie, Q.Z. Wang, *Tetrahedron* 73 (2017) 272-277.
- [44] N. Mergu, M. Kim, Y.A. Son, *Spectrochim. Acta A* 188 (2018) 571-580.
- [45] X. Meng, D. Cao, Z. Hu, X. Han, Z. Li, W. Ma, *RSC Adv.* 8 (2018) 33947-33951.
- [46] G. Zhu, Y. Huang, C. Wang, L.X. Lu, T.M. Sun, M. Wang, Y.F. Tang, D.D. Shan, S.J. Wen, J.L. Zhu, *Spectrochim. Acta A* 210 (2019) 105-110.
- [47] X. Tang, Z. Zhu, R.J. Liu, L. Ni, Y. Qiu, J. Han, Y. Wang, *Spectrochim. Acta A* 211 (2019) 299-305.
- [48] S. Goswami, S. Das, K. Aich, D. Sarkar, T.K. Mondal, C.K. Quah, H.K. Fun, *Dalton T.* 42 (2013) 15113-15119.
- [49] A. Hakonen, *Anal. Chem.* 81 (2009) 4555-4559.
- [50] T. Lu, F.W. Chen, *J. Comput. Chem.* 33 (2012) 580-592.
- [51] C. Lee, W. Yang, R.G. Parr, *Phys. Rev. B.* 37 (1988) 785-789.
- [52] R.L. Martin, *J. Chem. Phys.* 118 (2003) 4775-4777.
- [53] A.V. Marenich, C.J. Cramer, D.G. Truhlar, *J. Phys Chem B.* 113 (2009) 6378-6396.
- [54] Y. Gong, H.F. Liang, *Sensor. Actuat. B-chem.* 241 (2017) 1294-1302.
- [55] M. Pannipara, A.G. Al-Sehemi, A. Irfan, M. Assiri, A. Kalam, Y. S. Al-Ammari, *Spectrochim. Acta A* 201 (2018) 54-60.
- [56] M. Das, M. Sarkar, *ChemistrySelect* 4 (2019) 681-692.
- [57] Y. Gong, H. F. Liang, *Spectrochim. Acta A* 211 (2019) 342-347.
- [58] S.A. Markarian, M.C. Aznaurvan, *Mol. Biol. Rep.* 39 (2012) 7559-7567.
- [59] M. Dhanushkodi, G.G.V. Kumar, B.K. Balachandar, S. Sarveswari, S. Gandhi, J. Rajesh, *Dyes Pigments* 173 (2020) 107897.

- [60] G.G.V. Kumar, M.P. Kesavan, G. Sivaraman, J. Annaraj, K. Anitha, A. Tamilselvi, S. Athimoolam, B. Sridhar, J. Rajesh, *Sensor. Actuat. B-chem.* 2555 (2018) 3235-3247.
- [61] G.G.V. Kumar, R.S. Kannan, T.C.K. Yang, J. Rajesh, G. Sivaraman, *Anal. Methods* 11 (2019) 901-906.
- [62] R. Bhaskara, G.G.V. Kumar, G. Sivaraman, J. Rajesh, S. Sarveswaria, *Inorg. Chem. Commun.* 104 (2019) 110-118.
- [63] G.G.V. Kumara, M.P. Kesavana, A. Tamilselvi, G. Rajagopal, J.D. Rajaa, K. Sakthipandian, J. Rajesha, G. Sivaraman, *Sensor. Actuat. B-chem.* 273 (2018) 305-315.
- [64] B. Zhao, Y. Xu, Q.G. Deng, K. Wei, F. Yue, L.Y. Wang, Y. Gao, *Tetrahedron Lett.* 57 (2016) 953-958.
- [65] Y.M. Zhu, Z. L. Wang, J. Yang, X. Xu, S. F. Wang, Z. C. Cai and H. J. Xu, *Chinese J. Org. Chem.* 39 (2019) 427-433

A novel acylhydrazone coumarin fluorescent chemosensor C^4 for determination of Ni^{2+} was designed and synthesized with lower detection limit (2.1×10^{-11} M). Water samples and cell imaging experiments illustrated that C^4 could be applied to the detection of practical samples and in living cells.



Highlights

1. A novel acylhydrazone coumarin fluorescent chemosensor for determination of Ni^{2+} was synthesized.
2. The experimental results revealed a low detection limit of 2.1×10^{-11} M with high selectivity and excellent sensitivity.
3. Water samples and cell imaging experiments illustrated that C^4 could be applied to the detection of practical samples and in living cells.

